The effect of exchange and correlation on the agreement between APW and LCAO Compton profiles and experiment

1989 J. Phys.: Condens. Matter 1 9357

(http://iopscience.iop.org/0953-8984/1/47/007)

J. Phys.: Condens. Matter 1 (1989) 9357–9367. Printed in the UK

The effect of exchange and correlation on the agreement between APW and LCAO Compton profiles and experiment

D A Cardwell† and M J Cooper
Department of Physics, University of Warwick, Coventry CV4 7AL, UK

Received 26 May 1989, in final form 17 July 1989

Abstract. The formulation of an exchange and correlation correction based on that proposed by Lam and Platzman to theoretical Compton profiles calculated within the local-density approximation is described. This correction is evaluated for Al, Fe, Cr, Ni and V and compared with the differences between existing APW and LCAO calculations and experiment. Improved agreement between the corrected theoretical data and measured profiles is observed for both models. The APW method is found to be somewhat more successful in the formulation of electron momentum densities for good free-electron and transition-metal elements.

1. Introduction

In recent momentum density studies the occupation numbers of the high-order momentum states calculated within the local-density approximation (LDA) have consistently produced underestimates compared to those deduced from Compton scattering experiments; see for example, Rollason *et al* (1987) on nickel, Cardwell *et al* (1989) on chromium and Cooper (1985) or Williams (1977) for general reviews. In consequence poor agreement has been observed between the individual measured and calculated Compton profiles $J(p_z)$. This quantity is the one-dimensional projection of the momentum density $n(\boldsymbol{p})$ along a specific crystallographic direction labelled z in equation (1):

$$J(p_z) = \iint n(\boldsymbol{p})\, \mathrm{d}p_x\, \mathrm{d}p_y. \tag{1}$$

In particular, theoretical profiles have overestimated significantly the observed peak height. This discrepancy has been attributed to the neglect of exchange and correlation effects in the theoretical data. Since the effect of exchange and correlation on calculated Compton profiles is to promote electrons from low- to high-momentum states, the band theories that omit this consideration in their formulation of momentum density underestimate the width of the Compton profile and overestimate the peak height $J(0)$, because of the normalisation condition $\int_{-\infty}^{+\infty} J(p_z)\, \mathrm{d}p_z = N$, the number of electrons per atom.

† Present address: Allen Clark Research Centre, Plessey Research Caswell Limited, Towcester, Northants NN12 8EQ, UK.

0953-8984/89/479357 + 11 $02.50

This paper evaluates an exchange and correlation correction reported by Lam and Platzman (1974) and compares its results with the differences between published experimental and theoretical Compton profiles for several metals. This substantially resolves the residual discrepancies outlined above and facilitates a critical assessment of Compton profiles calculated within the LDA.

2. Density functional theory

The momentum density, $n(\boldsymbol{p})$, for interacting electrons in the Hartree–Fock approach is derived from the Fourier transform of the real-space one-electron wavefunctions, $\psi_i(\boldsymbol{r})$, i.e.

$$n(\boldsymbol{p}) = \sum_{i=1}^{N} |\langle \boldsymbol{p}|\psi_i(\boldsymbol{r})\rangle|^2 \tag{2}$$

where $\langle \boldsymbol{p}|$ represents a plane-wave state and the sum is over all the electrons. The Compton profile is then obtained from the $n(\boldsymbol{p})$ according to equation (1). Various band calculations have been applied to model $n(\boldsymbol{p})$ for many elements and compounds. Of these perhaps the most appropriate is that based on density functional theory (DFT; see Hohenberg and Kohn 1964). DTF is an exact ground-state formulation for the treatment of an inhomogeneous, interacting electronic distribution and is therefore applicable to Compton scattering studies of the ground-state momentum density.

In formulating the real-space ground-state wavefunction, DTF assumes that the total ground-state energy, which can be written as a unique functional of the charge density, may be expressed as a sum of the kinetic, $E^{\mathrm{KE}}_{[\rho(r)]}$, and Hartree, $E^{\mathrm{H}}_{[\rho(r)]}$, energies (the latter describing the classical electrostatic interaction amongst the conduction electrons and between the conduction electrons and the core) of a particular electronic system, plus whatever is left over, i.e.

$$E_{[\rho(r)]} = E^{\mathrm{KE}}_{[\rho(r)]} + E^{\mathrm{H}}_{[\rho(r)]} + E^{\mathrm{XC}}_{[\rho(r)]}. \tag{3}$$

Here $E^{\mathrm{XC}}_{[\rho(r)]}$ is, by definition, the exchange and correlation energy describing the spin-dependent interactions between electrons in the distribution. The exchange interaction, which arises as a consequence of the Pauli exclusion principle, is included in the Hartree–Fock method (see Fock 1930a, b). Correlation, on the other hand, is a collective term used to describe the spin-dependent interactions not included in the Hartree–Fock formulation (such as the interaction between electrons of anti-parallel spin, for example). The effects of exchange and correlation are incorporated in DFT by modification of the usual Hartree potential, $V^{\mathrm{H}}_{[\rho(r)]}$, in which case the effective potential, $V^{\mathrm{eff}}_{[\rho(r)]}$ corresponding to a total energy $E_{[\rho(r)]}$ can be written as

$$V^{\mathrm{eff}}_{[\rho(r)]} = V^{\mathrm{H}}_{[\rho(r)]} + V^{\mathrm{XC}}_{[\rho(r)]} \tag{4}$$

where $V^{\mathrm{XC}}_{[\rho(r)]}$ represents the exchange–correlation potential and $V^{\mathrm{H}}_{[\rho(r)]}$ is of the usual form, i.e.

$$V^{\mathrm{H}}_{[\rho(r)]} = V(\boldsymbol{r}) + \tfrac{1}{2}\int \frac{\rho(r)}{|\boldsymbol{r}-\boldsymbol{r}'|}\,\mathrm{d}\boldsymbol{r}'. \tag{5}$$

$V(\boldsymbol{r})$ is the external lattice potential. Minimisation of the total energy with respect to the

charge density, $\rho(\boldsymbol{r})$, then yields the self-consistent Kohn–Sham equations (see Kohn and Sham 1965) which may be written in the form

$$[-\nabla^2 - V^{\text{eff}}_{[\rho(\boldsymbol{r})]}(\boldsymbol{r})]\,\psi_i(\boldsymbol{r}) = \varepsilon_i \psi_i(\boldsymbol{r}). \tag{6}$$

It should be noted, however, that the minimisation procedure used to derive equation (6) is only defined for the ground-state energy and the charge density. Thus the set of orthonormal functions $\{\psi_i(\boldsymbol{r})\}$ do not correspond explicitly to the individual electron wavefunctions.

To extend DTF further it is necessary to relate the exchange–correlation energy to $V^{\text{XC}}_{[\rho(\boldsymbol{r})]}$. This is achieved from the minimisation procedure employed to derive the Kohn–Sham equations and yields the following expression:

$$V^{\text{XC}}_{[\rho(\boldsymbol{r})]} = \delta E^{\text{XC}}_{[\rho(\boldsymbol{r})]}/\delta\rho(\boldsymbol{r}). \tag{17}$$

Hence $V^{\text{XC}}_{[\rho(\boldsymbol{r})]}$ corresponds to the functional derivative of the exchange–correlation energy, from which the exchange–correlation term in the Kohn–Sham equation can be fully determined.

2.1. The local-density approximation

The residual problem with DFT is that the total exchange and correlation energy is not known explicitly and must therefore be approximated. This model-dependent quantity is the only approximation made in the Kohn–Sham formalism and its evaluation is central to the development of DFT.

Approximations to $E^{\text{XC}}_{[\rho(\boldsymbol{r})]}$ are usually made within the local-density approximation (LDA) such that

$$E^{\text{XC}}_{[\rho(\boldsymbol{r})]} = \int \varepsilon^{\text{h}}_{\rho_0}\rho(\boldsymbol{r})\,\mathrm{d}r \tag{8}$$

where $\varepsilon^{\text{h}}_{\rho_0}$ is the contribution of exchange and correlation to the total energy per particle in a homogeneous, interacting electron gas of constant density ρ_0.

The LDA assumes that $E^{\text{XC}}_{[\rho(\boldsymbol{r})]}$ consists of a sum of the individual contributions, $\varepsilon^{\text{h}}_{\rho_0}$, over the spatial extent of the inhomogeneous gas and determines each one by treating the distribution as if it were locally uniform. To calculate these contributions it is convenient to parametrise the electron density such that $\rho_0 = 3/4\pi r_{\text{s}}^3$ where r_{s} is the mean electron radius (i.e. the Wigner radius) and this uniquely determines the properties of the homogeneous electron gas. Observing that $\varepsilon^{\text{h}}_{\rho_0}$ assumes its maximum value in the low-density limit, an analytic fit to the exchange and correlation energy has been made by Gunnarson and Lundqvist (1976). Their fit is determined uniquely by r_{s}, which is consistent with the development of DFT, and has been applied successfully to a variety of electron distributions (see Lundqvist and March 1983).

Within the LDA the solutions to the Kohn–Sham equations would be exact when applied to a uniform electron gas if $\varepsilon^{\text{h}}_{\rho_0}$ can be deduced. In practice, therefore, the applicability of the LDA to real systems appears to be confined to distributions where the electron density is relatively slowly varying (i.e. those in which the range of $V^{\text{XC}}_{[\rho(\boldsymbol{r})]}$ is small compared with r_{s}). The local approximation, however, has been found to represent accurately electron distributions where $\rho(\boldsymbol{r})$ varies rapidly, for example over the region of an atomic core. This can be explained by the observation of Lundqvist and March (1983) that the contribution of exchange to the total energy of an electronic system is in general dominant over that of correlation. The same authors also showed that the range

of the exchange–correlation hole calculated via the LDA is similar to its true value. The exchange-correlation energy, therefore, is relatively insensitive to variations in charge density.

The most important feature of the local-density approximation with regard to momentum density studies, however, is that the effects of exchange and correlation on the Compton profile may be described by a correction term which may be simply added to the results of a given band calculation provided the local potential is known. This will be shown in the following section.

2.2. The Lam–Platzman correction

The charge density $\rho(\boldsymbol{r})$ can be deduced accurately and directly within the DFT formulation. However, the procedure for the deduction of the ground-state momentum density from the Kohn–Sham solutions is not so straightforward. For non-interacting or interacting electron distributions in the Hartree–Fock approximations, respectively, it can be shown that (see Lundqvist and March 1983)

$$n(p) = \sum_{i=1}^{N} |\langle \boldsymbol{p}|\chi_i(\boldsymbol{p})\rangle|^2 \tag{9}$$

where $\chi_i(\boldsymbol{p})$ are the Fourier transforms of the real-space one-electron wavefunctions. By application of Feynman's theorem, Lam and Platzman (1974) showed that, for the transformed solutions to the Kohn–Sham equations, $\chi_i(p)$, equation (9) becomes modified by the addition of an extra term, i.e.

$$n^{\mathrm{DFT}}_{[\rho(r)]}(\boldsymbol{p}) = \sum_{i=1}^{N} |\langle \boldsymbol{p}|\chi_i(\boldsymbol{p})\rangle|^2 + \frac{\delta E^{\mathrm{XC}}_{[\rho(r)]}}{\delta \varepsilon_p} \tag{10}$$

where the correction term is given by the derivative of the total exchange–correlation energy with respect to the individual electron energies arising from correlations between the states $|\chi_i(p)\rangle$. In the LDA this term becomes

$$\frac{\delta E^{\mathrm{LDA}}_{[\rho(r)]}}{\delta \varepsilon_p} = \int \frac{\delta \varepsilon^{\mathrm{h}}_{\rho_0}}{\delta \varepsilon_p} \rho(\boldsymbol{r})\, \mathrm{d}r \tag{11}$$

for which Lam and Platzman proposed the following ansatz:

$$\frac{\delta E^{\mathrm{LDA}}_{[\rho(r)]}}{\delta \varepsilon_p} = \int_{\text{unit cell}} (n^{\mathrm{h}}_{[\rho(r)]}(\boldsymbol{p}) - n^{\mathrm{f}}_{[\rho(r)]}(\boldsymbol{p}))\, \rho(\boldsymbol{r})\, \mathrm{d}r \tag{12}$$

where the bracketed term represents the difference between the homogeneous-interacting and the free-electron gas momentum densities, defined by the local potential $\rho(\boldsymbol{r})$.

Both $n^{\mathrm{h}}_{[\rho(r)]}$ and $n^{\mathrm{f}}_{[\rho(r)]}$ are necessarily normalised to one electron. For a one-dimensional momentum distribution (i.e. the Compton profile) this reduces to

$$\Delta J^{\mathrm{LDA}}_{[\rho(r)]}(q) = \int_{\text{unit cell}} \rho(\boldsymbol{r})[J^{\mathrm{h}}_{[\rho(r)]}(q) - J^{\mathrm{f}}_{[\rho(r)]}(q)]\, \mathrm{d}^3 r. \tag{13}$$

This is the Lam–Platzman correction term which describes the effect of exchange and correlation on the Compton profile. Furthermore, since it is modelled within the LDA, it is necessarily isotropic. For Compton profiles calculated from the wavefunction set

$\{\chi_i(\boldsymbol{p})\}$, this correction describes the adjustment necessary for the physical interpretation of the momentum distribution within the LDA, provided the charge density employed is common to both terms in equation (10).

3. Calculation of the Lam–Platzman correction

Accurate determination of the momentum-space occupation numbers corresponding to the quasi-particle properties of a homogeneous, interacting electron gas requires the evaluation of the electron self-energy as a function of wavevector (see Lundqvist 1968). From this the single-particle spectral weight function, commonly used to describe the plasmon spectra of an electron gas (see Lundqvist 1967), can be obtained and integrated with respect to energy to yield $n(\boldsymbol{k})$. This calculation is greatly simplified by the assumption of the random-phase approximation (RPA), in which each Fourier component of the effective potential can be treated independently—see Lundqvist (1968). It is difficult to identify the extent to which two existing calculations of the momentum density of a homogeneous interacting electron gas agree since only graphical data are available in each case (see Daniel and Vosko 1960, Lundqvist 1968). The two calculations appear to differ by up to ~3.5% at the extremes of $n(p)$ (i.e. at $p/p_F = 0$ and ~1.4, although good agreement is observed at $p \sim p_F$, where p_F is the Fermi momentum of the interacting electron gas). Bauer and Schneider (1983a), however, have pointed out that the Lundqvist occupation numbers are the more reliable of the two since those of Daniel and Vosko are calculated only to first order in the Hamiltonian. Consequently only the results at $p \sim p_F$ in the latter calculation are used in the momentum-density model presented here.

3.1. Momentum-density model

An analytic fit to the results of Lundqvist (1968) has been made in preference to an interpolation of the graphical data. The advantage of this method is that the conduction-electron contribution to $\Delta J^{\mathrm{LDA}}_{[\rho(r)]}$ can be calculated directly for any value of r_s.

The first analytic fit to $J^{n}_{[\rho(r)]} - J^{f}_{[\rho(r)]}$ was made by Rennert (1981). This fit has been subsequently modified according to the following equations:

$$\begin{aligned} n(p) &= 1 - a_{\rho_0}p^2 - \delta(1-p) && \text{for } p < p_F \\ &= a_{\rho_0}(b_{\rho_0} - p)^2/(b_{\rho_0} - 1)^2 && \text{for } p > p_F \end{aligned} \tag{14}$$

where

$$a_{\rho_0} = 1.7\alpha_{\rho_0} = 1.7/\pi^2 k_F. \tag{15}$$

b_{ρ_0} is the point at which $n(p)$ drops to zero and is a functional of the charge density. This parameter is determined by the following normalisation condition:

$$\int n(p)\, \mathrm{d}^3p = (4\pi/3)\, p_F^3. \tag{16}$$

δ corresponds to the deviation of the momentum density from unity at $p = 0$ for non-zero values of r_s and is obtained from the Lundqvist data; a_{ρ_0}, and hence b_{ρ_0} via equations (14) and (15), are calculated from the interstitial electron data of Moruzzi *et al* (1978). Together these parameters completely characterise the momentum distribution. The

Table 1. Characteristic parameters of the momentum density for varying amounts of correlation, r_s, calculated analytically with the delta approximation (equation (14)). The point at which the distribution intersects the p_z axis, b_ρ, is dependent on the degree of correlation and is invariably greater than that calculated by Rennert (1981) which is fixed at 1.4760.

r_s (Å)	p_F (au)	α_{ρ_0}	δ	b_{ρ_0} (p/p_F)
1.0	1.9192	0.0280	0.0110	1.5128
2.0	0.9596	0.0560	0.0220	1.5128
3.0	0.6397	0.0839	0.0390	1.5914
4.0	0.4798	0.1119	0.0560	1.5227
5.0	0.3838	0.1399	0.0720	1.5240
6.0	0.3199	0.1679	0.0864	1.5240

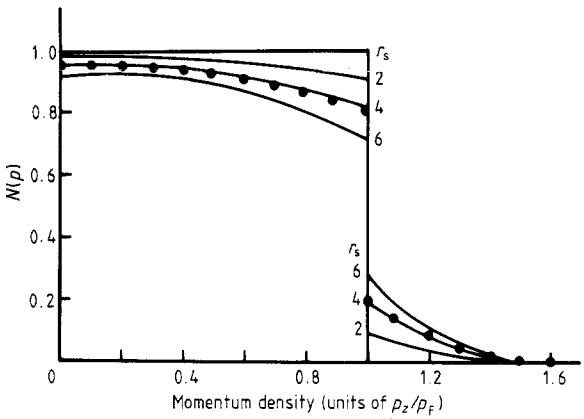

Figure 1. The momentum density in units of p/p_F calculated for $r_s = 2$, 4 and 6 from the analytic fit described by equations (14) and (15). The full circles correspond to $n(p)$ for $r_s = 4$ and are derived from the full self-energy calculation of Lundqvist (1968).

values of a_{ρ_0}, b_{ρ_0}, δ and p_F for the first six integral values of r_s are presented in table 1 and the corresponding momentum densities for $r_s = 2$, 4 and 6 Å are plotted in figure 1. The full circles represent the Lundqvist data for $r_s = 4$ which are in good agreement with the modelled distribution.

The input data for the Lam–Platzman correction were obtained by subtracting the free-electron Compton profile, which takes the form of an inverted parabola, from that derived from equation (14). Since both the interacting and free-electron Compton profiles were normalised to unity, the resulting difference has zero area in all calculations.

The input parameters required to calculate the Lam–Platzman correction for both core and conduction electrons are all taken from the tabulated data of Moruzzi *et al* (1978). The contributions to $\Delta J^{\mathrm{LDA}}_{[\rho(r)]}$ were calculated from the total electron density in the core region and the interstitial region and then summed. To simplify the calculation over the muffin-tin region, where the electrons are tightly bound, the contribution to the correction from each point in the core charge density was obtained by interpolating between $r_s^{\max}$ and 0 (i.e. the free-electron limit). Hence the input $J^{\mathrm{h}}_{[\rho(r]}(q) - J^{\mathrm{f}}_{[\rho(r)]}(q)$ appropriate to the core electrons was calculated for the spherically symmetric core-electron distribution of minimum charge density, i.e. the point at which the effects of exchange and correlation are the most significant. The determination of $r_s^{\max}$ therefore formed the basis of the calculations of the core contribution to $\Delta J^{\mathrm{LDA}}_{[\rho(r)]}$.

Table 2. Input parameters for the Lam–Platzman correction for Al, V, Cr, Fe and Ni.

Element	Z	Structure	a_0 (au)	r_s (au)	p_F (au)	Intersitital electrons per atom	Muffin-tin radius (au)
Aluminium	13	FCC	7.60	2.11	0.906	0.716	2.687
Vanadium	23	BCC	5.54	1.80	1.064	1.106	1.959
Chromium	24	BCC	5.30	1.71	1.121	1.134	1.874
Iron	26	BCC	5.15	1.71	1.123	1.044	1.821
Nickel	28	FCC	6.55	1.83	1.051	0.715	2.316

The conduction-electron contribution to the Lam–Platzman correction was calculated assuming the interstitial charge density to be constant. Consequently the input for the difference profile did not vary with r and was deduced for the exact conduction-electron charge density, ρ_0, according to the structure and valency of the element.

The input parameters for the Lam–Platzman correction of Al, V, Cr, Fe and Ni are given in table 2.

4. Results and discussion

4.1. The form of the correction

The results of the calculations are listed in table 3. The form of the correction in each case consists of a negative region in the vicinity of the origin, a sharp peak near the Fermi momentum and a high-momentum tail. It can be seen from figure 2, which compares the input profile difference calculated from the free-electron data in Morruzi *et al* (1978) with the Lam–Platzman corrections for aluminium, that the shape of $\Delta J^{\mathrm{LDA}}_{[\rho(r)]}$ is similar to $J^{\mathrm{h}}_{[\rho(r)]} - J^{\mathrm{f}}_{[\rho(r)]}$ but is of greater magnitude at all points of the distribution. This is because the input difference is normalised to one electron and becomes magnified when integrated over the unit cell. The high-momentum tail is an exclusive feature of the core-electron distribution and arises as a consequence of the large Fermi momentum associated with the high charge density at low r (see Moruzzi *et al* 1978).

Since the Lam–Platzman correction includes the core and conduction-electron contributions, it is difficult to relate a general trend in the above features to a specific input parameter. It is apparent, however, that the magnitude of $\Delta J^{\mathrm{LDA}}_{[\rho(r)]}$ at the origin is inversely proportional to the average charge density of the core. For metals such as aluminium, therefore, where the core charge density at high r is relatively low, the resultant correction exhibits a large dip at the origin which is consistent with the association of high exchange and correlation effects with low electron densities.

The conduction-electron contribution to $\Delta J^{\mathrm{LDA}}_{[\rho(r)]}$ varies typically from ~25% at the origin to ~40% at $p \sim p_F$. This is because a unique Fermi momentum is associated with the conduction-electron gas (of assumed constant charge density) and this gives rise to a strong positive peak at $p \sim p_F$. The core charge density, on the other hand, varies over the muffin-tin region with successive points in r space corresponding to different values of Fermi momenta for the equivalent electron gas. In essence the high- and low-momentum features of the Lam–Platzman correction are dominated by the core charge density, whereas the intermediate form of $\Delta J^{\mathrm{LDA}}_{[\rho(r)]}$ is determined to a greater extent by the distribution of the conduction electrons.

Table 3. The unconvolved Lam–Platzman correction for aluminium, vanadium, chromium, iron and nickel.

p_z (au)	Al	V	Cr	Fe	Ni
0.0	−0.098	−0.084	−0.074	−0.070	−0.075
0.1	−0.098	−0.084	−0.074	−0.070	−0.075
0.2	−0.096	−0.083	−0.073	−0.069	−0.074
0.3	−0.091	−0.081	−0.071	−0.068	−0.072
0.4	−0.083	−0.077	−0.069	−0.065	−0.069
0.5	−0.069	−0.071	−0.064	−0.061	−0.065
0.6	−0.047	−0.062	−0.058	−0.056	−0.057
0.7	−0.013	−0.048	−0.048	−0.047	−0.046
0.8	0.038	−0.029	−0.034	−0.035	−0.031
0.9	0.110	−0.001	−0.015	−0.017	−0.009
1.0	0.111	0.037	0.012	0.006	0.020
1.1	0.060	0.067	0.046	0.047	0.043
1.2	0.025	0.048	0.053	0.046	0.037
1.3	0.006	0.030	0.038	0.034	0.024
1.4	0.002	0.018	0.024	0.022	0.015
1.5	0.001	0.011	0.015	0.014	0.009
1.6	0.000	0.009	0.010	0.009	0.006
1.8	0.001	0.008	0.008	0.006	0.005
2.0	0.001	0.009	0.007	0.006	0.005
2.5	0.003	0.011	0.009	0.007	0.005
3.0	0.004	0.012	0.010	0.008	0.006
3.5	0.004	0.011	0.010	0.009	0.007
4.0	0.004	0.007	0.009	0.008	0.008
5.0	0.004	0.002	0.003	0.006	0.007
6.0	0.003	0.001	0.001	0.002	0.004
7.0	0.001	0.001	0.001	0.001	0.001
10.0	0.000	0.001	0.001	0.001	0.001

4.2. Comparison with previous calculations and experiments

The application of the Lam–Platzman correction to the results of DFT calculations always results in a shift of electron density from low to high momenta. The extent of this shift reflects the degree to which the core and conduction electrons are correlated. In addition to the results presented here, this has also been observed in a study of copper by Bauer and Schneider (1983b) and in a study of nickel by Rollason *et al* (1987).

Those earlier calculations of the Lam–Platzman term are less accurate than the results presented here. This is because former authors calculated the correction term from a single input for $J^{h}[\rho(r(] - J^{f}[\rho(r)]$ corresponding to the Lundqvist occupation numbers for $r_s = 2$. Subsequent interpolation of these data for $2 < r_s < 0$ over both the core and conduction-electron regions introduced discrepancies. Consequently a difference of ~0.3% $J(0)$ at the origin and ~0.2% $J(0)$ at $p \sim 1$ au for the nickel correction is observed between the present Lam–Platzman correction and that derived by Rollason *et al*. At the other points in $\Delta J^{\mathrm{LDA}}_{[\rho(r)]}$, however, good agreement is observed between the two calculations.

Figure 3 shows the difference between APW (Wakoh *et al* 1976) and LCAO (Rath *et al* 1973) theory and experiment for the nearest-neighbour directional Compton profiles of (*a*) iron (see Rollason *et al* 1983a), (*b*) vanadium (Rollason *et al* 1983b), (*c*) nickel

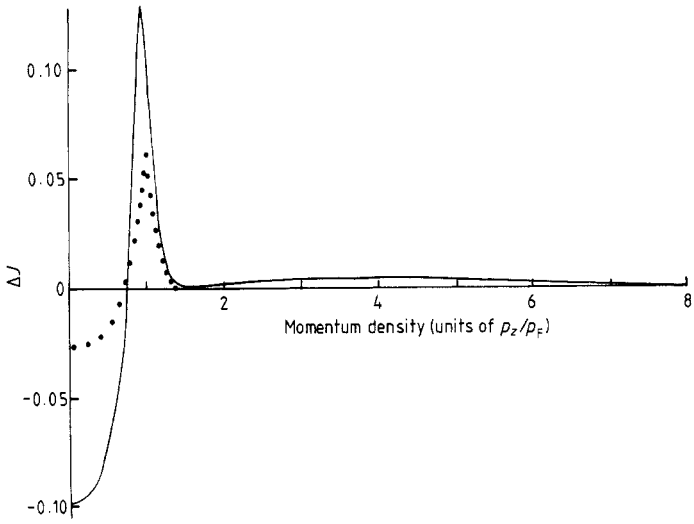

Figure 2. The Lam–Platzman correction for aluminium (full curve). The full circles show the change in the Compton lineshape of aluminium when interactions are introduced into a homogeneous electron gas, i.e. $J^{h}_{[\rho(r)]} - J^{i}_{[\rho(r)]}$ derived from the analytical fit of Rennert (1981) discussed in § 3.1, using the parameters listed in tables 1 and 2. The magnitude of the correction should be compared with a peak height of 4 electrons per au at the origin.

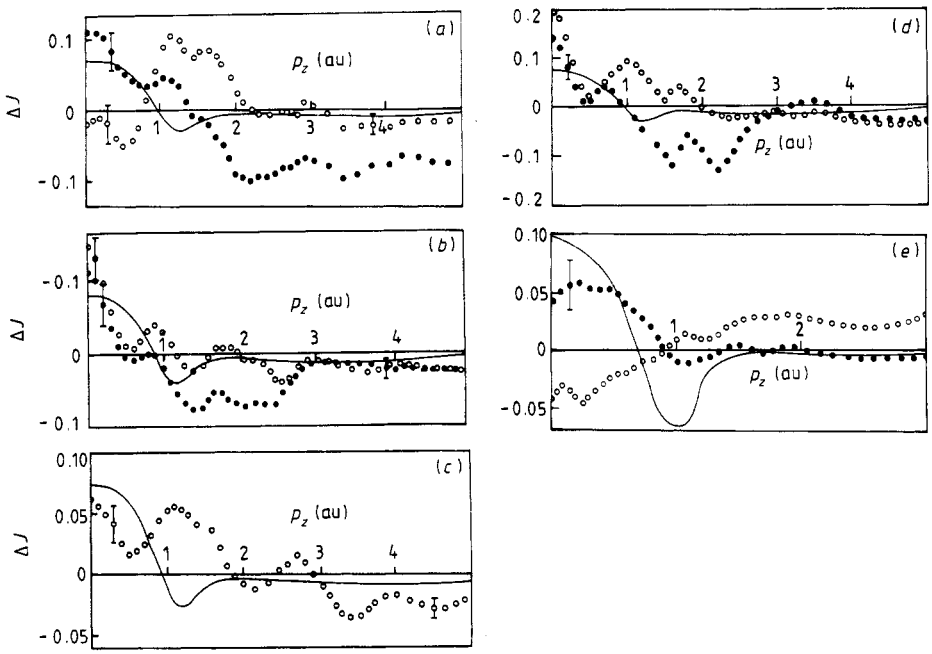

Figure 3. Theory minus experiment for the nearest-neighbour Compton profiles of (*a*) iron [111] (Rollason *et al* 1983a), (*b*) vanadium [111] (Rollason *et al* 1983b), (*c*) nickel [110] (see Rollason *et al* 1987), (*d*) chromium [111] (Cardwell *et al* 1989) and (*e*) aluminium [110] (Cardwell and Cooper 1986). In each case the full and open circles correspond to the results of the APW and LCAO band calculations, respectively. The full curve represents the inverted Lam–Platzman correction convoluted with a gaussian of FWHM 0.4 au. It should be subtracted from the difference data, i.e. this curve would fit the data curves if agreement were perfect.

(Rollason *et al* 1987), (*d*) chromium (Cardwell *et al* 1989) and (*e*) aluminium (Cardwell and Cooper 1986). The appropriate Lam–Platzman correction, convoluted with a gaussian of FWHM 0.4 au to represent the instrumental response function, is shown in each case by the full curve. In this figure the correction has been inverted for ease of comparison. It has not been applied to the difference data directly since the potential employed in their construction is not identical to that used in the band calculations.

4.3. APW and LCAO models

A complicating problem with the existing APW band calculations is that their predicted Compton profiles are deficient in electron density. This discrepancy, which arises because $J(\boldsymbol{p})$ is deduced by integrating $n(\boldsymbol{p})$ over a limited momentum range in these particular studies, is manifest predominantly at high-momentum states. Hence the conduction-electron contribution to the Compton profile is restricted typically to values of momentum less than 10 au in the APW data discussed here. This problem is less significant for aluminium, because the conduction electrons have a lower occupation density of the higher-order momentum states than for the 3d transition metals. In the latter it amounts to a deficit in the area under the Compton profiles of approximately 0.2 electrons.

The APW calculations all employed a core charge density derived from a DFT formulation. Since a similar $\rho(\boldsymbol{r})$ was used in calculating the Lam–Platzman term, a significant improvement in the agreement between experiment and theory for all the APW difference data shown is observed. This is evidenced by the fact that the corrections plotted in figure 3 mimic very closely the differences between experiment and theory at low-momentum values where the correction term is most significant. In addition the sign of the correction is in good agreement with the 'APW − experiment' difference curves over the entire momentum range for all the elements shown. This suggests that the APW method is particularly appropriate for the calculation of the momentum density of both good free-electron and transition-metal elements.

The LCAO method uses trial wavefunctions more appropriate to core-electron states and its prediction of the Compton profiles of metals is slightly less successful than its application to localised systems. This is apparent in the data shown in figure 3 where, with the exception of V, the differences between experiment and theory are greater than those observed for the APW curves at low momenta. In addition, the sign of the correction does not follow that of the 'LCAO − experiment' curves as well as it does in the case of the APW data. The errors associated with the data are too large to discriminate conclusively between the two models, but the APW model is slightly favoured.

Both APW and LCAO theory minus experiment difference curves exhibit oscillations in the data after the correction has been applied. It has been shown in the case of copper and chromium (see Bauer and Schneider (1983b) and Cardwell (1987) respectively) that these occur with the frequency of the reciprocal lattice. Since this corresponds to a build-up in momentum density at points around the primary and secondary Fermi surfaces, the isotropic Lam–Platzman correction cannot account for their presence. A method of modelling a directional correlation correction has been proposed by Wakoh and Matsumoto (1989) who have applied it successfully to chromium (see Cardwell *et al* 1989). The formulation of a directional correction, based on the local-density approximation, will be the subject of a future publication.

In conclusion it is evident that the agreement between experiment and theory for APW- and LCAO-based band calculations can be improved significantly by inclusion of

exchange and correlation effects in the latter. The resulting agreement between APW results and experiment is marginally better than for LCAO. Agreement between the predictions of theory and experimental results has, for the first time, been observed consistently at low values of momentum. Thus the problem associated with determining momentum densities from the solutions of the Kohn–Sham equations appears to have been overcome by the application to theoretical data of an independently formulated Lam–Platzman correction. This provides an improved basis for assessing the relative merits of various band techniques in Compton scattering experiments.

Acknowledgments

We would like to acknowledge the many informative and invaluable discussions with Dr A J Rollason, Dr D Laundy, Dr J B Staunton and Professor S Wakoh throughout this period of research. In addition we are grateful to the SERC for the provision of a research studentship (DAC) during the tenure of which this research was conducted.

References

Bauer G E W and Schneider J R 1983a *Solid State Commun.* B **47** 673
—— 1983b *Z. Phys.* B **54** 17
Cardwell D A 1987 *PhD Thesis* University of Warwick
Cardwell D A and Cooper M J 1986 *Phil. Mag.* B **54** 37
Cardwell D A, Cooper M J and Wakoh S 1989 *J. Phys.: Cond. Matter* **1** 541
Cooper M J 1985 *Rep. Prog. Phys.* **48** 415
Daniel E and Vosko S H 1960 *Phys. Rev.* **20** 2041
Fock V Z 1930a *Z. Phys.* **61** 126
—— 1930b *Z. Phys.* **62** 795
Gunnarson O and Lundqvist B L 1976 *Phys. Rev.* B **13** 4274
Hohenberg P and Kohn W 1964 *Phys. Rev.* **136** B864
Kohn W and Sham L J 1965 *Phys. Rev.* A **140** 1133
Kubo Y, Wakoh S and Yamashita J 1976 *J. Phys. Soc. Japan.* **41** 830
Lam L and Platzman P 1974 *Phys. Rev.* B **9** 5122
Lundqvist B I 1967 *Phys. Kondens. Materie* **6** 193, 206
—— 1968 *Phys. Kondens. Materie* **7** 117
Lundqvist S and March N H (ed.) 1983 *Theory of the Inhomogeneous Electron Gas* (New York: Plenum)
Matsumoto M 1989 private communication
Moruzzi V L, Williams A R and Janak J F 1978 *Calculated Electronic Properties of Metals* (New York: Pergamon)
Rath J, Wang C S, Tawil R A and Callaway J 1973 *Phys. Rev.* B **8** 5139
Rennert P 1981 *Phys. Status Solidi* b **105** 567
Rollason A J, Holt R S and Cooper M J 1983a *J. Phys. F: Met. Phys.* **13** 1807
—— 1983b *Phil. Mag.* B **47** 51
Rollason A J, Schneider J, Laundy D, Holt R S and Cooper M J 1987 *J. Phys. F: Met. Phys.* **17** 1105
Wakoh S and Kubo Y 1977 *J. Magn. Magn. Mater.* **5** 202
Wakoh S, Kubo Y and Yamashita J 1976 *J. Phys. Soc. Japan* **40** 1043
Wakoh S and Matsumoto M 1989 *J. Phys.: Condens. Matter* **1** at press
Williams B G (ed.) 1987 *Compton Scattering* (London: McGraw-Hill)